Organic & Biomolecular Chemistry

PAPER

View Article Online
View Journal | View Issue

A coumarin-quinolinium-based fluorescent probe for ratiometric sensing of sulfite in living cells†

Cite this: *Org. Biomol. Chem.*, 2014, **12**, 4637

Li Tan, Weiying Lin,* Sasa Zhu, Lin Yuan and Kaibo Zheng

Received 18th January 2014,
Accepted 2nd May 2014

DOI: 10.1039/c4ob00132j

www.rsc.org/obc

Based on a novel coumarin-quinolinium platform, probe **2** was rationally designed and synthesized as a novel ratiometric fluorescent sensor for sulfite anions. The probe exhibited a wide dynamic concentration range for sulfite anions in a PBS buffer (containing 1 mg mL^{-1} BSA). More importantly, the probe was suitable for ratiometric fluorescence imaging in living cells with high sensitivity, favorable selectivity, and minimal cytotoxicity.

Introduction

With the development of industries, sulfur dioxide (SO_2) is an inevitable product of the combustion of coal and fossil fuels and has had a detrimental effect on the environment. Numerous epidemiological studies have implied that frequent exposure to SO_2 not only induces many respiratory responses,[1] but is also related to lung cancer, cardiovascular diseases, and neurological disorders, such as migraine headaches, strokes, and brain cancer.[2] Furthermore, when SO_2 is dissolved in solution or after inhalation, it is hydrated and an equilibrium is formed between two anions: sulfite and bisulfite. Sulphite, because of its antioxidant and preservative properties, is commonly used to prevent food from browning, discourage bacterial growth in wines, and maintain the stability and potency of some medications.[3] However, exposure to high doses of sulfite may cause adverse reactions and acute symptoms, including dermatitis, urticaria, flushing, hypotension, abdominal pain, and diarrhoea.[4] In fact, there is evidence that some people may be extremely sensitive to sulfite even at very low levels,[5] and that bronchoconstriction can occur in many asthmatic patients.[6] Besides, toxicological studies also suggest that SO_2 and its derivatives could change the characteristics of voltage-gated sodium channels and potassium channels in rat hippocampal neurons[7] and affect thiol levels, which can break the redox balance in cells[8] and produce a neuronal insult.[9] In view of the seriousness of the consequences of sulphite exposure, the Joint FAO/WHO Expert Committee on Food Additives has regulated an acceptable daily intake of sulfite to be lower than 0.7 mg kg^{-1} of body weight.[10] So far, several analytical techniques including the official Monier-Williams methods,[11] electrochemistry,[12] spectrophotometry,[13] chromatography,[14] capillary electrophoresis,[15] and titration[16] have been developed to detect sulfites in food and beverages. However, these methods usually require tedious sample and reagent preparation or complicated instruments, and therefore are not suitable for routine analysis. As an alternative, fluorescence sensing is appealing because of its high sensitivity, excellent selectivity, and simplicity. Furthermore, fluorescence sensing is potentially applicable for bioimaging in living cells and offers temporal and spatial resolution. Basically, molecular fluorescence probes detecting biological species are based on the unique increase or decrease of the emission intensity signal. A major limitation of intensity-based probes is that variations in the sample environment and probe distribution may be problematic for utilization in quantitative measurements.[17] By contrast, ratiometric fluorescent probes allow the measurement of emission intensities at two different wavelengths, which should provide a built-in correction for environmental effects and can also increase the dynamic range of fluorescence measurements.[18]

Up to now, several fluorescent probes for sulfites have been designed on the basis of the selective deprotection of a levulinate group,[19] complexation with amines,[20] selective reaction with aldehyde[21] and Michael-type additions.[22] However, most of these fluorescent probes respond to sulfites with changes only in fluorescent intensity; thus, it is still a challenge to develop ratiometric fluorescent probes for sulfite. On the other hand, coumarins, to the best of our knowledge, are a classic type of a push–pull dye, in which the intramolecular charge transfer (ICT) process from the electron donor to the acceptor proceeds upon excitation. Typically, for efficient ICT, the donor and acceptor are located in the 7- and 3-position, respectively.[23] We envisioned that diethylamino moieties at the

State Key Laboratory of Chemo/Biosensing and Chemometrics, College of Chemistry and Chemical Engineering, Hunan University, Changsha, Hunan 410082, P. R. China. E-mail: weiyinglin2013@163.com; Fax: (+)86-0731-88821464

†Electronic supplementary information (ESI) available: Experimental procedures, characterization data, and additional spectra. See DOI: 10.1039/c4ob00132j

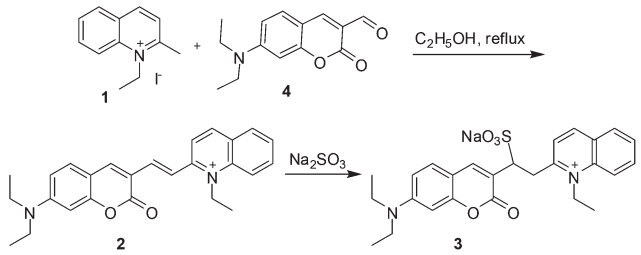

Scheme 1 Design and synthesis of probe **2** as a new ratiometric fluorescent sulphite probe.

7-position and quinolyl moieties at the 3-position would be a desirable coumarin push–pull system for an ICT process. Therefore, we designed and synthesized probe **2** (Scheme 1) as a novel ratiometric fluorescent sulfite probe based on a coumarin-quinolinium platform.

Results and discussion

Probe **2** was readily synthesized in two steps (Scheme 1). A mixture of 2-methylquinoline with ethyl iodide yielded *N*-ethyl-2-methylquinolinium iodide **1** in 87% yield,[24] which was then condensed with 7-(diethylamino)-2-oxo-2*H*-chromene-3-carbaldehyde in anhydrous ethanol to give target probe **2**. The structures of the synthesized compounds were fully characterized by standard NMR and mass spectrometry.

With probe **2**, we evaluated its spectral properties in the absence or presence of sulfite in an aqueous buffer (pH 7.4, 25 mM PBS buffer with 30% ethanol) (Fig. S1†). The response of probe **2** towards sulfite was very good. Considering its application in living systems, we checked the spectral response of probe **2** (5 μM) to sulphite in pure PBS buffer at ambient temperature (Fig. S2†). The results showed that probe **2** had weak fluorescent intensity, which may be due to its limited solubility. Therefore, we added bovine serum albumin (BSA at 1 mg mL^{-1}) in a PBS buffer solution.[25] As displayed in Fig. S3,† the free ratiometric probe **2** exhibited a main absorption band at around 515 nm, and almost no absorption appeared at 410 nm, consistent with the ICT signalling mechanism. However, the addition of SO_3^{2-} induced a large blue shift in the absorption peak, indicating the formation of a new species upon the treatment of probe **2** with SO_3^{2-}. In good agreement with the absorption findings, the probe exhibited a ratiometric fluorescent response to the SO_3^{2-} anion. We chose the isosbestic point (450 nm) as the optimal excitation wavelength. Upon excitation at 450 nm, the free sensor displayed an intense emission band at 610 nm. However, as shown in Fig. 1, fluorescent ratios of probe **2** at 508 and 610 nm (I_{508}/I_{610}) showed a large change from 0.34 to 4.81 upon treatment with the SO_3^{2-} anion. The emission ratios (I_{481}/I_{659}) were linearly proportional to the amount of sulfite (0.15–75 μM) (Fig. 2) with a detection limit (S/N = 3) of 8.9×10^{-8} M in PBS buffer (pH 7.4, containing 1 mg mL^{-1} BSA), suggesting that the probe is potentially

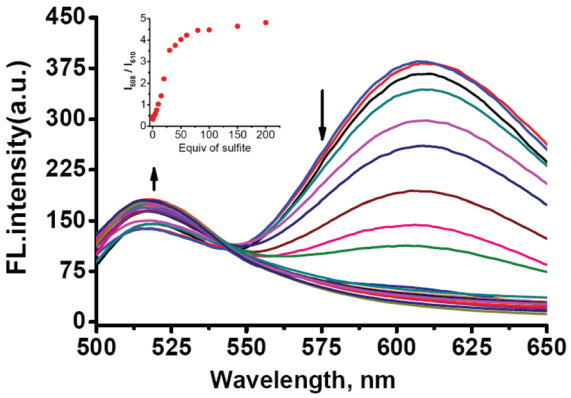

Fig. 1 Fluorescence spectra of probe **2** (5 μM) in PBS buffer (pH 7.4, containing 1 mg mL^{-1} BSA) in the presence of SO_3^{2-} (0–200 equiv.) with excitation at 450 nm. Inset: fluorescence intensity ratio (I_{508}/I_{610}) of probe **2** changes (5.0 μM) with the amount of Na_2SO_3.

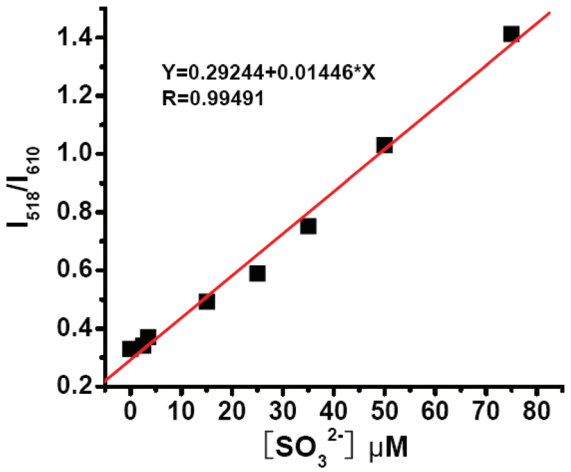

Fig. 2 Plot of the fluorescent ratio (I_{508}/I_{610}) of probe **2** in PBS buffer (pH 7.4, containing 1 mg mL^{-1} BSA) as a function of the sulfite concentration (0–200 equiv.).

useful for the quantitative determination of sulfite concentrations in a large dynamic range and has high sensitivity in living systems.

To shed light on the SO_3^{2-}-induced fluorescence ratiometric response, we decided to characterize the addition product and carried out theoretical calculations. First, the product of probe **2** + Na_2SO_3 was isolated and then subjected to NMR analysis. The partial ^{1}HNMR spectra of probe **2** and the isolated compound **3** are shown in Fig. 3. The resonance signal corresponding to the alkene proton H_{2b} at 8.52 ppm (doublet) disappeared, and a new peak at 4.43 ppm (triplet) assigned to the proton H_{3b} emerged. The addition of sulfite to C=C resulted in the formation of a chiral center of C_{3b}, with the nonequivalent protons of the methylene group at C_{3a}. Therefore, the signal for H_{2a} at 8.17 ppm (doublet) shifted to a higher field and appeared as two peaks at 3.77 ppm (dd) and 4.08 ppm (dd), respectively. At the same time, the resonance signal of H_{2c} at 8.47 ppm shifted to 8.275 ppm, due to the

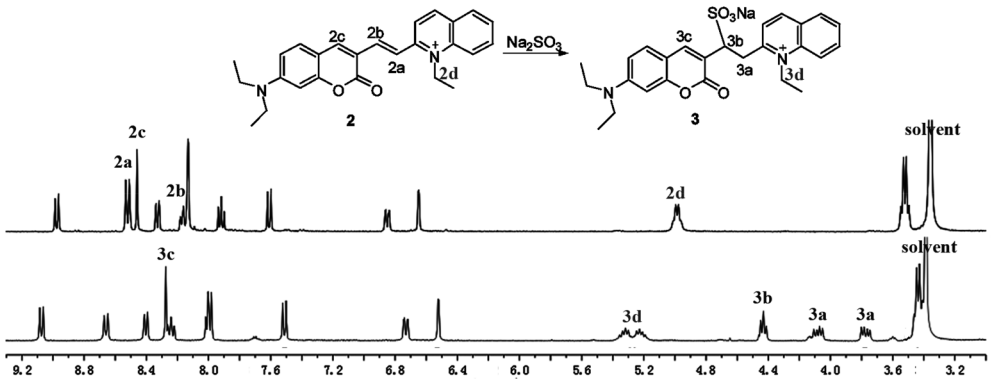

Fig. 3 Partial ^{1}H NMR spectra of probe **2** and isolated compound **3** in DMSO-d_6.

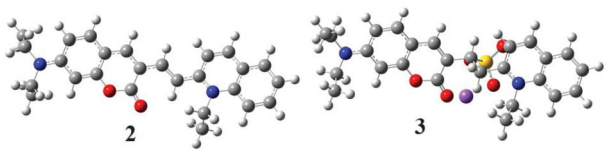

Fig. 4 DFT optimized structures of **2** and **3**. In the ball-and-stick representation, carbon, nitrogen, oxygen, and sulphur atoms are colored in gray, blue, red and yellow, respectively.

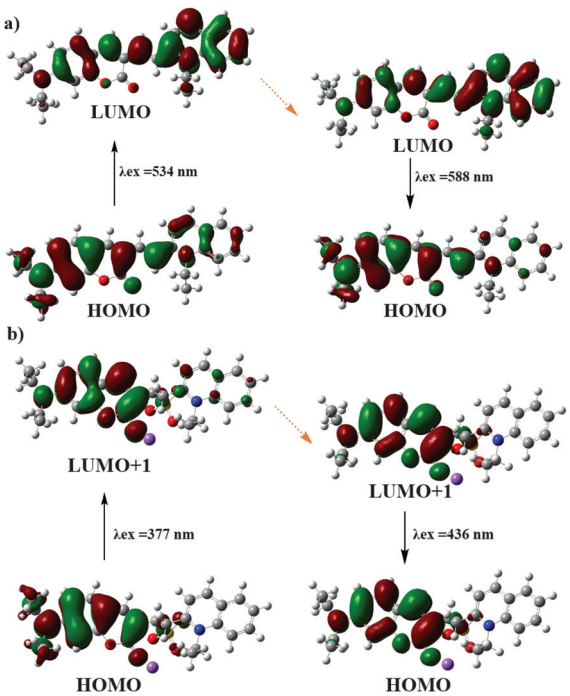

Fig. 5 Frontier molecular orbital plots of **2** (a) and **3** (b) in water (CPCM model) involved in the vertical excitation (*i.e.*, UV/Vis absorption, left column) and emission (right column). The vertical-excitation-related calculations are based on the optimized geometry of the ground state (S_0), and the emission-related calculations are based on the optimized geometry of the excited state (S_1). Excitation and radiative processes are marked as solid lines, and the non-radiative processes are marked by dotted lines.

shielding effect of the adjacent alkyl group. The results are in good agreement with that of the reported paper.[22] To better understand the mechanism of probe **2**'s response to sulfite, density functional theory (DFT) and time-dependent DFT (TD-DFT) by the Gaussian 09 program were employed to explain the distinctions in the spectral profiles of probe **2** and compound **3** (in water solvent at the B3LYP/6-31+G(d) (PCM) level). The optimized structures in the ground states of **2** and **3** are shown in Fig. 4. The quinolyl and coumarinyl moieties of **2** were well coplanar *via* a conjugated bridge (–C=C–), and the dihedral angle between the quinolyl and coumarinyl moieties was less than 1° (Fig. 4). The addition of sulfite to the double bond of the conjugated bridge inhibited the addition of quinolyl and coumarinyl moieties, and the dihedral angle for reaction product **3** was 84° (Fig. 4). This structural difference between **2** and **3** showed the significant difference in π-conjunction between **2** and **3**. We then further compared the highest occupied molecular orbital (HOMO) and the lowest unoccupied molecular orbital (LUMO) of probe **2** and compound **3** in the ground and excited states. In the case of free probe **2**, the electronic transition was mainly contributed by a HOMO–LUMO transition. The π electrons on the LUMO of probe **2** were mainly located on the quinolyl moiety, but the HOMO was mostly positioned at the coumarin unit (Fig. 5a). Thus, an ICT took place through the conjugated bridge between the coumarin and quinolinium groups. In addition, TDDFT calculations indicated that probe **2** showed the absorption peak at 534 nm (f = 1.3175) and a high fluorescence band at 588 nm (f = 0.9409). However, the electronic transition of **3** was mainly contributed by the HOMO–LUMO+1 transition. The π electrons on both the HOMO and LUMO+1 in the ground state were mainly located on the π-conjugated coumarin framework (Fig. 5b). Thus, the ICT process of compound **3** was weaker than that of probe **2**, which could lead to a blue shift in the absorption and fluorescence spectra. TDDFT calculations indicated that compound **3** showed the absorption peak at 377 nm (f = 0.6475) and a weak fluorescence band at 436 nm (f = 0.0029), which was in good agreement with the observation that the measured absorption and emission wavelengths of compound **3** were shorter than those of probe **2**. Furthermore, the π electrons on the

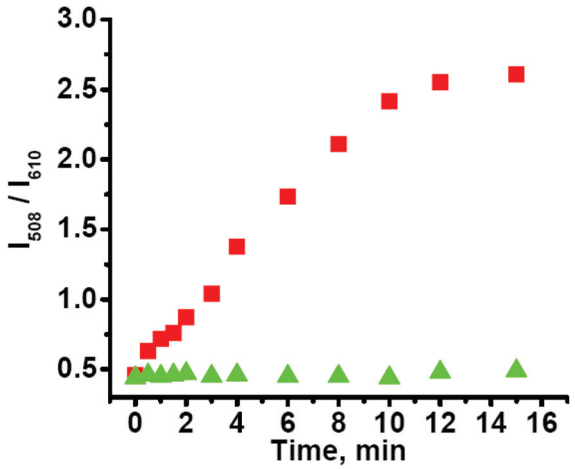

Fig. 6 Reaction time profiles of probe **2** (5.0 μM) in the absence [▲] or presence of 20 equiv. of Na_2SO_3 [■]). The fluorescent intensities ratio I_{508}/I_{610} were continuously monitored at time intervals in PBS buffer (pH 7.4, containing 1 mg mL^{-1} BSA). Time points represent 0, 0.5, 1, 1.5, 2, 3, 4, 6, 8, 10, 12 and 15 min.

HOMO/LUMO+1 of compound **3** were mainly distributed on coumarin moieties, while those on the LUMO were located on the quinoline moiety (Fig. S4†). Thus, upon the excitation of compound **3**, a process of *d*-PET involving the transfer of one electron from the excited coumarin moieties to the quinoline moieties leads to the fluorescence of compound **3** being partially quenched, which explained the observation that the measured emission intensity of compound **3** was weaker than that of probe **2**.

The time profile of the fluorescence response of probe **2** (5.0 μM) in the presence of SO_3^{2-} (20 equiv.) in pH 7.4 PBS buffer (containing 1 mg mL^{-1} BSA) are displayed in Fig. S5,† showing that the response of probe **2** to sulfite was very quick. Fig. 6 shows the fluorescence intensity ratio I_{508}/I_{610} of probe **2** towards SO_3^{2-} (20 equiv.) at time intervals from 0 to 15 min, with the pseudo-first-order kinetics constant calculated as k_{obs} = 0.128 min^{-1} (Fig. S6†).

To investigate the selectivity, probe **2** (5.0 μM) was treated with various biologically relevant species, including CH_3COO^-, I^-, Br^-, Cl^-, F^-,CO_3^{2-}, N_3^-, NO_2^-, $H_2PO_4^-$, NO_3^-, SO_4^{2-}, SCN^-, $S_2O_3^{2-}$, S^{2-}, Vc, Cys, GSH and SO_3^{2-} in pH 7.4 PBS buffer (containing 1 mg mL^{-1} BSA). As exhibited in Fig. 7, the representative species CH_3COO^-, I^-, Br^-, Cl^-, F^-, CO_3^{2-}, N_3^-, NO_2^-, $H_2PO_4^-$, NO_3^-, SO_4^{2-}, SCN^-, $S_2O_3^{2-}$, Vc, Cys, and GSH were prepared at 1 mM, and S^{2-} was prepared at 150 μM. Notably, all these relevant species displayed no response to probe **2** (Fig. 7). By contrast, upon treatment of Na_2SO_3 (100 μM) with the probe, a large fluorescence ratiometric signal was observed. Thus, these data demonstrate that probe **2** is highly selective for SO_3^{2-} over the other biological species tested, including over glutathione (GSH) and cysteine at the biologically relevant concentrations, validating the hypothesis that the SO_3^{2-}-triggered addition reaction is chemoselective for SO_3^{2-} over other biological species. The selectivity of probe **2** was superior or comparable to already known fluorescent

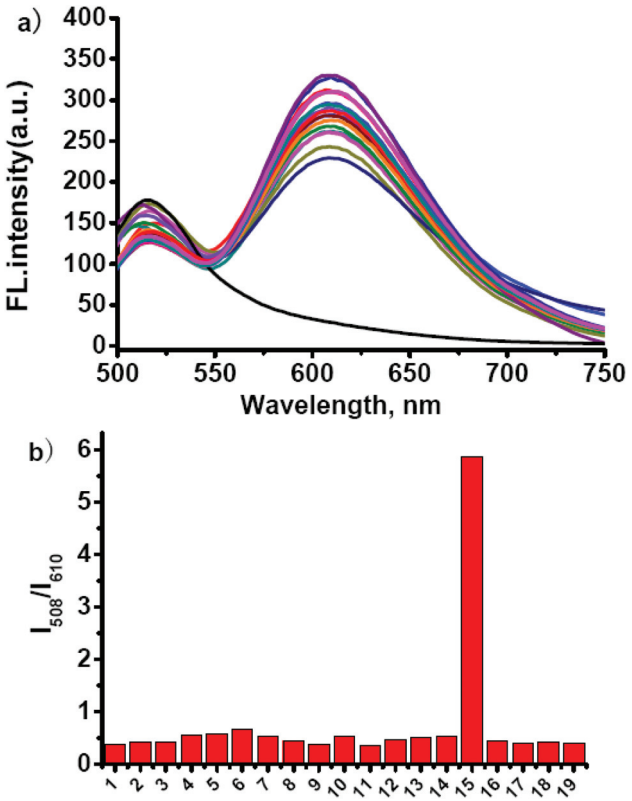

Fig. 7 Fluorescent spectra (a) and ratio I_{508}/I_{610} (b) of probe **2** (5.0 μM) to various biologically relevant species in PBS buffer (pH 7.4, containing 1 mg mL^{-1} BSA). Red bars represent the addition of the excess of representative species. 1. Blank, 2. CH_3COO^-, 3. I^-, 4. Br^-, 5. Cl^-, 6. cys, 7. N_3^-, 8. NO_2^-, 9. $H_2PO_4^-$, 10. F^-, 11. NO_3^-, 12. SO_4^{2-}, 13. SCN^-, 14. $S_2O_3^{2-}$, 15. SO_3^{2-}, 16. S^{2-}, 17. Vc, 18. CO_3^{2-}, 19. GSH.

SO_3^{2-} probes. In addition, we further examined the absorption and fluorescence response of the probe toward Na_2SO_3 in the presence of other potentially competing species. The other species only displayed minimum interference (Fig. S7†). This suggests that probe **2** is potentially useful for sensing Na_2SO_3 in the presence of other related species in pH 7.4 PBS buffer (containing 1 mg mL^{-1} BSA).

We envision that the desirable water solubility, high sensitivity, and favorable selectivity of probe **2** should benefit the ratiometric imaging of SO_3^{2-} anion in biological samples with high resolution. First, the MTT assays were conducted for probe **2** at different concentrations, and the results showed that probe **2** had low cytotoxicity after a long period (24 h) (Fig. S8†), suggesting that the probe was desirable for imaging applications in living cells. Therefore, we performed a ratiometric fluorescence imaging experiment for SO_3^{2-} anion in living cells. The fluorescence ratio image of the intracellular SO_3^{2-} anion with probe **2** is shown in Fig. 8. RAW 264.7 macrophage cells incubated with probe **2** for 30 min showed a weak emission ratio (F_{blue}/F_{red}) (Fig. 8b), which indicated that probe **2** could penetrate the cell. When cells pre-treated with probe **2** were further incubated with exogenous Na_2SO_3 in PBS for 30 min and washed, a notable emission ratio (F_{blue}/F_{red}) enhancement was observed (Fig. 8d). These preliminary experi-

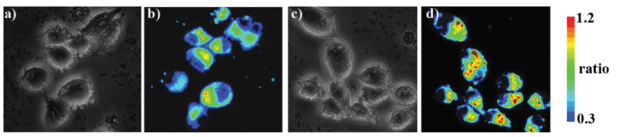

Fig. 8 Fluorescence images of RAW 264.7 macrophage cells. (a and b) Cells incubated with probe **2** (2 μM) for 30 min: (a) bright-field transmission image and (b) fluorescent ratio (F_{blue}/F_{red}) image generated from the blue and red channels. (c and d) Cells incubated with probe **2** (2 μM) for 30 min after preincubation with 100 μM Na_2SO_3 for 30 min: (c) bright-field transmission image, and (d) fluorescence ratio (F_{blue}/F_{red}) image generated from the blue and red channels.

mental results demonstrated that probe **2** could be applied for the ratiometric imaging of SO_3^{2-} in biological samples with high resolution.

Conclusions

In summary, we presented a novel probe based on a coumarin-quinolinium platform. This novel probe could be used as a ratiometric fluorescence sensor for SO_3^{2-} anions with high sensitivity, favorable selectivity, as well as a wide dynamic concentration range in a PBS buffer solution (containing 1 mg mL^{-1} BSA). More importantly, the probe is permeable to the cell membrane and can image living cells with low cytotoxicity. We expect that this design concept will be further developed for the detection of SO_2 derivatives for food safety, clinical and environmental applications.

Experiment section

Materials and instruments

Unless otherwise stated, all reagents were purchased from commercial suppliers and used without further purification. The solvents used were purified by standard methods prior to use. Twice-distilled water was used in all experiments. Mass spectra were performed using an LCQ Advantage ion trap mass spectrometer from Thermo Finnigan or an Agilent 1100 HPLC/MSD spectrometer. NMR spectra were recorded on an INOVA-400 spectrometer using TMS as an internal standard. Electronic absorption spectra were obtained on a Labtech UV Power PC spectrometer. Photoluminescence spectra were recorded at room temperature with a HITACHI F4600 fluorescence spectrophotometer with a 1 cm standard quartz cell. pH measurements were carried out on a Mettler-Toledo Delta 320 pH meter. Cell imaging was performed with an inverted microscope. TLC analysis was performed on silica gel plates, and column chromatography was conducted over silica gel (mesh 200–300), both of which were obtained from Qingdao Ocean Chemicals.

DFT calculations

The ground state structures of **2** and **3** were optimized using DFT with a B3LYP functional and 6-31G(d) basis set. The initial geometries of the compounds were generated by Gaussview software. Excited state calculations (UV-vis absorption) were carried out with time dependent DFT (TDDFT) with the optimized structure of the ground (DFT/6-31G(d)). The emission of the fluorophores was calculated on the basis of the optimized S_1 excited state geometry. All of these calculations were performed with Gaussian 09 (Revision A.02).[26]

Preparation of the test solution

The stock solution of probe **2** was prepared at 0.5 mM in DMSO. The solutions of various test species were prepared from CH_3COONa, KI, KBr, NaCl, NaF, Na_2CO_3, NaN_3, $NaNO_2$, KH_2PO_4, KNO_3, $NaSO_4$, KSCN, $Na_2S_2O_3$, Na_2S, $C_6H_5Na_3O_7$, GSH, cysteine and Na_2SO_3 in the twice-distilled water. The test solution of probe **2** (5.0 μM) in 3 mL 25 mM PBS buffer pH 7.4 PBS buffer (containing 1 mg mL^{-1} BSA) was prepared by placing 0.03 mL of the probe **2** stock solution and 3.0 mL of the aqueous buffer with dissolved BSA (1 mg mL^{-1}). The resulting solution was shaken well and incubated with appropriate testing species for 30 min at 25 °C before recording the spectra. Unless otherwise noted, for all measurements, the excitation wavelength was 450 nm, the excitation slit widths were 10 nm, and emission slit widths were 10 nm.

RAW 264.7 macrophage cells culture and imaging using probe 2

Raw 264.7 murine macrophages were obtained from the Third Xiangya Hospital and cultured in DMEM (Dulbecco's Modified Eagle Medium) supplemented with 10% FBS (fetal bovine serum) in an atmosphere of 5% CO_2 and 95% air at 37 °C. Immediately before the experiments, the cells were washed with PBS, followed by incubating with probe **2** (2 μM) for 30 min at 37 °C (in PBS containing 0.5% DMSO) and then by washing with PBS three times and imaged.

Cytotoxicity assays

RAW 264.7 macrophage cells were cultured in DMEM supplemented with 10% FBS (fetal bovine serum) in an atmosphere of 5% CO_2 and 95% air at 37 °C. Immediately before the experiments, the cells were placed in a 96-well plate, followed by the addition of increasing concentrations of probe **2** (99.9% DMEM and 0.1% DMSO). The final concentrations of the probe were kept from 0.5 to 10 μM (n = 3). The cells were then incubated at 37 °C in an atmosphere of 5% CO_2 and 95% air at 37 °C for 24 h, followed by MTT assays. An untreated assay with DMEM (n = 3) was also conducted under the same conditions.

Synthesis of *N*-ethyl-2-methylquinolinium iodide 1

Compound **1** was prepared according to the reported reference. A mixture of 2-methylquinoline (1.2 mmol) and ethyl iodide (1.5 mmol) in 30 ml of toluene was heated at reflux for 20 h. The crude product was filtered and recrystallized from absolute ethanol, washed with ether and dried under vacuum to give compound **1** (yield 87.1%) as a yellow powder, which was used for the next step reaction without further purifi-

cation. ^{1}H NMR (400 MHz, d_6-DMSO) δ 1.55 (t, J = 7.2 Hz, 3H), 3.14 (s, 3H), 5.02 (q, J = 7.2 Hz, 2H), 8.01 (t, J = 7.4 Hz, 1H), 8.16 (d, J = 8.8 Hz, 1H), 8.25 (t, J = 8.0 Hz, 1H), 8.44 (d, J = 8.0 Hz, 1H), 8.64 (d, J = 8.0 Hz, 1H), 9.13 (d, J = 8.4 Hz, 1H); ^{13}C NMR (100 MHz, d_6-DMSO) δ 13.94, 22.92, 47.71, 119.35, 126.05, 128.72, 129.50, 131.10, 135.76, 138.53, 146.07, 161.00; MS (ESI): [M^+] 172.1; HRMS m/z calcd for $C_{26}H_{27}N_2O_2$ [M^+]: 172.1121. Found 172.1129.

Synthesis of probe 2

1-Ethyl-2-methylquinolinium iodide **1** (59.8 mg, 0.2 mmol) was treated with coumarin 7-(diethylamino)-2-oxo-2*H*-chromene-3-carbaldehyde (49.1 mg, 0.2 mmol) in anhydrous ethanol (10 mL). The reaction mixture was then refluxed for 10 h, and the solvent was removed under reduced pressure. The resulting residue was purified by column chromatography on silica gel (CH_2Cl_2 to CH_2Cl_2–acetone = 50 : 1) to yield the product as a purple powder (78.7 mg, yield: 74.8%). Mp 139–140 °C. ^{1}H NMR (400 MHz, d_6-DMSO) δ 1.15–1.18 (t, J = 7.2 Hz, 6H), 1.63 (t, J = 7.6 Hz, 3H), 3.49–3.54 (q, 4H), 4.96–5.01 (q, 2H), 6. 64 (d, J = 2.0 Hz, 1H), 6.83–6.86 (dd, J = 8.8 Hz, 2.0 Hz, 1H), 7.59–7.62 (d, J = 8.8 Hz, 1H), 7.89–7.94 (t, J = 8.4 Hz, 1H), 8.13–8.18 (m, 3H), 8.31–8.33 (d, J = 8.0 Hz, 1H), 8.46(s, 1H), 8.50–8.53 (d, J = 9.2 Hz, 2H), 8.96–8.98 (d, J = 8.8 Hz, 1H); ^{13}C NMR (100 MHz, d_6-DMSO) δ 12.70, 13.91, 44.80, 46.93, 96.57, 108.87, 110.79, 113.33, 116.84, 118.94, 120.82, 128.07, 128.95, 130.59, 131.69, 135.27, 138.36, 143.84, 143.88, 147.92, 153.01, 155.61, 157.09, 159.99. MS (ESI): [M^+] 399.1; HRMS m/z calculated for $C_{26}H_{27}N_2O_2$ [M^+]: 399.2067. Found 399.2056.

Synthesis of compound 3

Probe **2** (20.0 mg, 0.05 mmol) dissolved in 3 mL ethanol was treated with a Na_2SO_3 (63.0 mg, 0.5 mmol) solution and stirred at room temperature for 30 min. The solution was evaporated under vacuum, and the resulting residue was then subjected to preparative thin layer chromatography (CH_2Cl_2–CH_3CH_2OH = 10 : 1) to give compound **3** (20.1 mg, 84.1% yield) as a yellow solid. ^{1}H NMR (400 MHz, d_6-DMSO) δ 1.12 (t, J = 6.0 Hz, 6H), 1.62 (t, J = 6.0 Hz, 3H), 3.41–3.46 (m, 4H), 3.76–3.80 (m, 1H), 4.41–4.45 (q, 1H), 4.43 (t, J = 8.0 Hz, 1H), 5.19–5.36 (m, 2H), 6.52 (d, 1H), 6.72–6.75 (m, 1H), 7.51 (d, J = 8.0 Hz, 1H), 7.98–8.02 (m, 2H), 8.22–8.28 (m, 2H), 8.40 (d, J = 8.0 Hz, 1H), 8.66 (d, J = 8.0 Hz, 1H), 9.07 (d, J = 8.0 Hz, 1H); ^{13}C NMR (100 MHz, d_6-DMSO) δ 12.53, 14.51, 37.58, 44.08, 57.10, 96.41, 108.09, 109.09, 117.06, 119.64, 125.15, 128.48, 129.49, 129.58, 130.85, 135.26, 137.92, 141.17, 145.37, 150.44, 155.48, 161.90, 162.04. MS (ESI): [M^+] 503.0.

Acknowledgements

This work was financially supported by NSFC (20972044, 21172063), NCET (08-0175), the Doctoral Fund of Chinese Ministry of Education (20100161110008), and the Fundamental Research Funds for the Central Universities, Hunan university.

Notes and references

1 S. Iwasawa, Y. Kikuchi, Y. Nishiwaki, M. Nakano, T. Michikawa, T. Tsuboi, S. Tanaka and T. Uemura, *J. Occup. Health*, 2009, **51**, 38–47.
2 N. Sang, Y. Yun, H. Li, L. Hou, M. Han and G. K. Li, *Toxicol. Sci.*, 2010, **114**, 226–236.
3 C. S. Pundir and R. Rawal, *Anal. Bioanal. Chem.*, 2013, **405**, 3049–3062.
4 (*a*) H. Vally, N. L. Misso and V. Madan, *Clin. Exp. Allergy*, 2009, **39**, 1643–1651; (*b*) H. Niknahad and P. J. O'Brien, *Chem.-Biol. Interact.*, 2008, **174**, 147–154.
5 (*a*) T. Oliphant, A. Mitra and M. Wilkinson, *Contact Dermatitis*, 2012, **66**, 128–130; (*b*) P. García-Ortega, E. Scorza and A. Teniente, *Clin. Exp. Allergy*, 2010, **40**, 688–690.
6 (*a*) H. Vally, P. J. Thompson and N. L. A. Misso, *Clin. Exp. Allergy*, 2007, **37**, 106–1066; (*b*) R. K. Bush, S. L. Taylor, K. Holden, J. A. Nordlee and W. W. Busse, *Am. J. Med.*, 1986, **81**, 816–820; (*c*) D. D. Stevenson and R. A. Simon, *J. Allergy Clin. Immunol.*, 1981, **68**, 26–32.
7 G. K. Li and N. Sang, *Ecotoxicol. Environ. Saf.*, 2009, **72**, 236.
8 L. Migliore and F. Coppedè, *Mutat. Res.*, 2009, **674**, 73–84.
9 N. Sang, Y. Yun, G. Yao, H. Li, L. Guo and G. Li, *Toxicol. Sci.*, 2011, **124**, 400–413.
10 W. J. FAO, in *WHO food additives series, 60*, ed. World Health Organization, Geneva, 2009.
11 G. W. Monier-Williams, *Analyst*, 1927, **52**, 343–344.
12 D. Huang, B. Xu, J. Tang, J. Luo, L. Chen, L. Yang, Z. Yang and S. Bi, *Anal. Methods*, 2010, **2**, 154–158.
13 (*a*) M. S. Abdel-Latif, *Anal. Lett.*, 1994, **27**, 2601–2614; (*b*) Y. Li and M. Zhao, *Food Control*, 2006, **17**, 975–980.
14 (*a*) L. Pizzoferrato, G. Di Lullo and E. Quattrucci, *Food Chem.*, 1998, **63**, 275–279; (*b*) R. F. McFeeters and A. O. Barish, *J. Agric. Food Chem.*, 2003, **51**, 1513–1517.
15 (*a*) Z. Daunoravicius and A. Padarauskas, *Electrophoresis*, 2002, **23**, 2439–2444; (*b*) G. Jankovskiene, Z. Daunoravicius and A. Padarauskas, *J. Chromatogr., A*, 2001, **934**, 67–73.
16 D. Lowinsohn and M. Bertotti, *Food Addit. Contam.*, 2001, **18**, 773–777.
17 (*a*) S.-R. Liu and S.-P. Wu, *Org. Lett.*, 2013, **15**, 878–881; (*b*) H. Yu, X. Zhang, Y. Xiao, W. Zou, L. Wang and L. Jin, *Anal. Chem.*, 2013, **85**, 7076–7084; (*c*) H. Y. Au-Yeung, J. Chan, T. Chantarojsiri and C. J. Chang, *J. Am. Chem. Soc.*, 2013, **135**, 15165–15173; (*d*) J. Liu, Y.-Q. Sun, Y. Huo, H. Zhang, L. Wang, P. Zhang, D. Song, Y. Shi and W. Guo, *J. Am. Chem. Soc.*, 2014, **136**, 574–577; (*e*) T. Guo, L. Cui, J. Shen, W. Zhu, Y. Xu and X. Qian, *Chem. Commun.*, 2013, **49**, 10820–11822; (*f*) F. Kong, R. Liu, R. Chu, X. Wang, K. Xu and B. Tang, *Chem. Commun.*, 2013, **49**, 9176–9178; (*g*) G. Li, D. Zhu, Q. Liu, L. Xue and H. Jiang, *Org. Lett.*, 2013, **15**, 2002–2005; (*h*) L. Long, L. Zhou, L. Wang, S. Meng, A. Gong, F. Dub and C. Zhang, *Org. Biomol. Chem.*, 2013, **11**, 8214–8220.
18 (*a*) C. Hu, W. Sun, J. Cao, P. Gao, J. Wang, J. Fan, F. Song, S. Sun and X. Peng, *Org. Lett.*, 2013, **15**, 4022–4025; (*b*) S. Goswami, S. Das, K. Aich, B. Pakhira, S. Panja,

S. K. Mukherjee and S. Sarkar, *Org. Lett.*, 2013, **15**, 5412–5415; (*c*) Q. Wan, Y. Song, Z. Li, X. Gao and H. Ma, *Chem. Commun.*, 2013, **49**, 502–504; (*d*) D. Zhai, S.-C. Lee, S.-W. Yunb and Y.-T. Chang, *Chem. Commun.*, 2013, **49**, 7207–7209.

19 (*a*) M. G. Choi, J. Y. Hwang, S. Y. Eor and S.-K. Chang, *Org. Lett.*, 2010, **12**, 5624–5627; (*b*) X. Gu, C. Liu, Y. Zhu and Y. Zhu, *J. Agric. Food Chem.*, 2011, **59**, 11935–11939; (*c*) S. Chen, P. Hou, J. Wang and X. Song, *RSC Adv.*, 2012, **2**, 10869–10873.

20 Y. M. Sun, C. Zhong, R. Gong, H. L. Mu and E. Q. Fu, *J. Org. Chem.*, 2009, **74**, 7943–7946.

21 C. Yu, M. Luo, F. Zeng and S. Wu, *Anal. Methods*, 2012, **4**, 2638–2640.

22 (*a*) M.-Y. Wu, T. He, K. Li, M.-B. Wu, Z. Huang and X.-Q. Yu, *Analyst*, 2013, **138**, 3018–3025; (*b*) Y.-Q. Sun, J. Liu, J. Zhang, T. Yang and W. Guo, *Chem. Commun.*, 2013, **49**, 2637–2639; (*c*) H.-Y. Tian, J.-H. Qian, Q. Sun, H.-Y. Bai and W.-B. Zhang, *Anal. Chim. Acta*, 2013, **788**, 165–170.

23 (*a*) G. Signore, R. Nifos, L. Albertazzi, B. Storti and R. Bizzarri, *J. Am. Chem. Soc.*, 2010, **132**, 1276–1288; (*b*) J. Wang, X. Qian and J. Cui, *J. Org. Chem.*, 2006, **71**, 4308–4311.

24 A. Bajorek, J. Kabatc and J. Pączkowski, *Dyes Pigm.*, 2009, **82**, 372–378.

25 (*a*) M. M. A. Sekar, P. D. Hampton, T. Buranda and G. P. López, *J. Am. Chem. Soc.*, 1999, **121**, 5135–5141; (*b*) H. Sunahara, Y. Urano, H. Kojima and T. Nagano, *J. Am. Chem. Soc.*, 2007, **129**, 5597–5604.

26 M. J. Frisch, *et al.*, *GAUSSIAN 09 (Revision A.02)*, Gaussian, Inc., Pittsburgh, PA, 2009.